https://arabjchem.org

ScientificScholar®
Knowledge is power
Publisher of Scientific Journals

Arabian Journal of Chemistry

2025 18 (12) 4982025

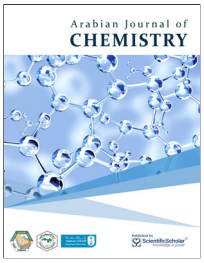

Original Article

Synthesis of itaconic acid-based non-isocyanate polyurethane coating with excellent heat insulation and corrosion resistance

Bin Chen, Xu Wang, Haoran Xu, Yu Zhang*, Chengqian Wang*

School of Petrochemical Technology, Jilin University of Chemical Technology, No. 45, Chengde Street, 132022, Jilin, China

ARTICLE INFO

Keywords:
Coating
Corrosion resistance
Itaconic acid
Non-isocyanate polyurethane

ABSTRACT

The objective of this study is to explore an environmentally friendly route for synthesizing non-isocyanate polyurethane (NIPU) coatings from renewable resources. A carbamate diol (CD10), featuring hydroxyl groups at both ends of the molecular chain, was synthesized by a melt ring-opening reaction using propylene carbonate (PC) and decanediamine (DDA). Due to the inherent rigidity and brittleness of CD10, it cannot form a high-performance coating independently. To address this limitation, biobased NIPUs were synthesized by incorporating itaconic acid (IA), a biobased material, as a soft chain segment into the CD10 structure. By varying the number of soft chain segments, it is possible to produce NIPUs coatings with tunable properties that cure naturally at room temperature without the need for curing equipment. The structure and physical properties of the NIPUs were characterized using Fourier transform-infrared (FT-IR), ^{1}H nuclear magnetic resonance (NMR), thermogravimetric analysis (TGA), thermal conductivity testing, water contact angle measurement, and pencil hardness testing. Additionally, their environmental stability was assessed by measuring water absorption in deionized water, acidic and alkaline solutions, and organic solvents. Additionally, their corrosion resistance in saltwater was evaluated. The results indicate that the coatings demonstrate significant performance due to the abundance of ester and urethane groups within the macromolecular chains of the NIPUs, leading to the formation of numerous intramolecular and intermolecular hydrogen bonds and an increase in cross-linking density. The potential application of these materials as film-forming agents for coatings, including heat-insulating and anticorrosive coatings, is promising. This study follows the concept of sustainable green development.

1. Introduction

Due to its excellent surface protection, chemical and abrasion resistance, mechanical properties, high elasticity, and good biocompatibility, polyurethane (PU) has emerged as one of the most versatile polymers. It is widely utilized across various industries, including furniture, automotive components, clothing, footwear, elastomers, coatings, as well as wall and roof insulation [1-4]. Despite the numerous advantages of conventional PUs, their drawbacks cannot be overlooked. Traditionally, PUs are synthesized from diisocyanates (or polyisocyanates) and polyols, in which the isocyanates are derived from petrochemical feedstocks. Moreover, the production of isocyanates requires the use of highly toxic phosgene, posing significant risks to both human health and the environment [5]. In contrast, non-isocyanate PUs (NIPUs) are synthesized without the use of toxic isocyanates, thereby eliminating the associated health and environmental hazards present in the conventional PU production process [6].

In this context, NIPUs or dihydroxycarbamates (DHUs) obtained through the polymerization of diamines and cyclic carbonates become promising alternatives to conventional PU, since this chemical reaction precludes the use of toxic phosgene and isocyanates in the production of polymers [7]. For example, DHUs are synthesized from cyclic carbonates such as ethylene carbonate (EC) [8,9] or propylene carbonate (PC) [10,11] with diamines such as hexane-1,6-diamine (HMDA) or isophorone diamine (IPDA) [12]. The reaction mechanism of cyclic carbonate and amine is initiated by the amine's nucleophilic attack on cyclic carbonate, followed by a deprotonation reaction, ultimately resulting in the formation of a DHU [13]. However, if NIPUs are synthesized by self-condensation of DHU alone, very rigid and easily broken NIPUs are formed [14,15]. To avoid these disadvantages, it is possible to introduce soft chain segments into the main chain of the polymer to improve its mechanical or other properties [16-18]. Furthermore, the bio-content of NIPUs can be significantly increased by employing monomers from renewable or bio-based feedstocks. Indeed, NIPUs and/or NIPU-based coatings have been previously reported [19-27], which are derived from vegetable oils [28], cashew nutshell liquids [29], lignocellulose [30], limonene [31], glycerol [32], succinic acid [33], itaconic acid (IA) [34], and the like. IA is one of the 12 important bio-based materials proposed by the U.S. Department of Energy because biotechnological production of IA from renewable feedstocks is feasible. IA contains a double bond and two carboxyl groups simultaneously, which gives it good structural regulatory ability and enables it to participate in various polymerization reactions. IA can be obtained by sugar fermentation. This process is green and environmentally friendly,

***Corresponding authors:**
E-mail addresses: wangchengqian1992@126.com (C. Wang), zhang99yu@jlict.edu.cn (Y. Zhang)

Received: 11 May, 2025 **Accepted:** 23 July, 2025 **Epub Ahead of Print:** 08 October 2025 **Published:** 14 November 2025
DOI: 10.25259/AJC_498_2025

which is in line with the concept of sustainable development. IA and its derivatives are widely used in the synthesis of unsaturated polyester, which is often used as a film-forming material of coatings [35-38].

Recently, an increasing number of researchers have explored the application of NIPUs in coating. Huang [38] *et al.* synthesized an itacon-based unsaturated polyester (IAF) from the biomass source (IA) and flame retardant (FRC-6) via the melting polycondensation reaction in one pot, and used different ratios of IAF, N-(hydroxymethyl) acrylamide (NMA), and γ-methylacryloxy propyl trimethoxysilane (MPS) as raw materials. A series of UV-curable hybrid coatings were prepared by UV-curable and sol-gel methods. The wood coated with UV-curable coatings showed excellent flame-retardant properties. IAF7N1Si2-W reached a UL-94 V-0 grade and limiting oxygen index (LOI) value of 33.7%, and effectively inhibited heat propagation and combustion degree. Ling [39] *et al.* successfully synthesized flax oil-based cyclic carbonate from flax oil, and developed a series of water-based flax oil-based NIPUs coatings, all of which showed excellent thermal stability and mechanical properties due to the combined influence of intermolecular hydrogen bonding and carbamate groups. Choong [40] *et al.* obtained the crosslinked coating through the acid-catalyzed transesterification reaction of hexa (methoxymethyl) melamine (HMMM) with NIPU hydroxyl group, showing good thermal stability (up to 245°C) and water resistance, and soaked the coated aluminum test piece in 5 wt% NaCl solution at 50°C for 5 days. The corrosion resistance of aluminum sheet significantly improved. J. Pouladi [41] *et al.* synthesized a non-isocyanate polyhydroxycarbamate network from linseed oil, in which the 75% carbonized coating showed the best corrosion resistance.

The objective of this study is to design and synthesize innovative bio-based NIPU coatings for thermal and corrosion protection via an environmentally friendly route. To fulfill the renewable/sustainable requirements, most chemicals used in this study are bio-based. The synthesis of NIPUs comprises three primary steps, as shown in Scheme 1: (i) In the first step, carbamate diol (CD10) is synthesized by melting ring-opening reaction of PC and decamethylene diamine (DDA) (ii) in the second step, the successfully synthesized CD10 is utilized as a hard chain segment along with varying amounts of the soft chain segment IA (the specific amounts of CD10 and IA have been detailed in Table 1). This mixture undergoes pre-polycondensation catalyzed by p-toluene sulfonic acid, with the primary objective being the removal of water generated during the reaction. (iii) In the third step, NIPU is synthesized via melt polycondensation, catalyzed by tin (II) isocrylate, a metal catalyst. Given that the soft segment consists entirely of IA, NIPUs exhibits complete solubility in anhydrous ethanol [42]. Therefore, NIPU is dispersed in anhydrous ethanol, configured as an emulsion, and naturally cures to a film at room temperature without the use of any specific curing equipment.

The resulting coatings were thoroughly analyzed and examined using Fourier transform-infrared (FT-IR) and ^{1}H nuclear magnetic resonance (NMR) to elucidate the molecular structure. Notably, many ester groups were found in the structural units of NIPUs, suggesting that extensive hydrogen bonding may exist in the synthesized polymer. Further research efforts focused on the effects of soft segment content

Table 1. The molar ratio of the raw materials for synthesizing NIPUs and the thermal properties of CD10, NIPUs, and WPU.

Sample	CD10[a] (mol)	IA[b] (mol)	$T_{5\%}$[c] (°C)	T_{max}[d] (°C)	Char yield at 700°C[e] (%)
CD10	—	—	259	292	0.09
$NIPU_{0.8}$	1	0.8	237	464	4.74
$NIPU_{0.9}$	1	0.9	227	468	4.96
$NIPU_{1.0}$	1	1.0	220	465	6.60
$NIPU_{1.1}$	1	1.1	218	466	8.84
$NIPU_{1.2}$	1	1.2	217	468	8.85
WPU	—	—	205	404	7.26

[a,b]The amount of hard segment (CD10) substance and the amount of soft segment (IA) substance required for the synthesis of NIPUs.
[c]Corresponding to 5% weight loss of polymers.
[d]Corresponding to the maximum derivative weight loss of polymers.
[e]The proportion of residual coke at 700°C.

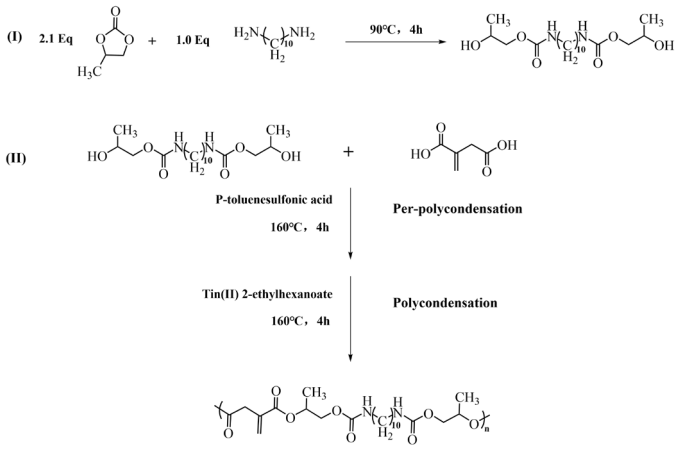

Scheme 1. (I) CD10 is generated by PC and sebacediamine, and (II) NIPU is generated by CD10 and IA.

and crosslinked network structure on key parameters of NIPU coating, such as thermal conductivity, corrosion resistance, water resistance, and thermal stability. Additionally, a series of tests, such as acid and alkali resistance, solvent resistance, pencil hardness, and adhesion, were conducted to provide a comprehensive understanding of the performance characteristics of NIPU coatings. This study follows the concept of sustainable green development.

2. Materials and Methods

2.1. Materials

Propylene carbonate (PC, 99%), 1,10-diaminodecane (DDA, 97%), itaconic acid (IA, AR, ≥99.0%), tin(II) 2-ethylhexanoate (95%), sodium chloride (NaCl, AR, 99.5%), and DMSO-d_6 (D, 99.9%) were purchased from Shanghai Macklin Biochemical Technology Co., Ltd. p-Toluenesulfonic acid (AR), sodium hydroxide (NaOH), acetonitrile (HPLC grade), and anhydrous ethanol (AR, ≥99.7%) were obtained from Tianjin Damao Chemical Reagent Factory. Hydrochloric acid (HCl, AR) was purchased from Tianjin Kaixin Chemical Industry Co., Ltd., and potassium bromide (KBr, AR) was supplied by Tianjin Guangfu Technology Co., Ltd. The waterborne PU (WPU) was purchased from Shenzhen Jitian Chemical Co., Ltd. All chemicals were used as received without further purification.

2.2. Synthesis of carbamate diol (CD10) and NIPUs

As demonstrated in Figure 1, the synthesis of the carbamate diol was conducted as follows: PC (21.44 g, 0.21 mol) and 1,10-diaminosilane (17.23 g, 0.1 mol) were introduced into a three-necked flask equipped with a condenser tube, a mechanical stirrer, and a nitrogen gas inlet. The reaction temperature was raised to 90°C and maintained for 4 h, with a continuous flow of nitrogen gas to prevent significant oxidation of the reactants. Upon completion of the reaction, the mixture was poured into anhydrous EtOH for recrystallization. The recrystallized product was subsequently placed in an oven at 60°C for 24 h, resulting in the formation of white solid powder CD10 after grinding.

As illustrated in Figure 1, CD10 was introduced into a three-necked flask equipped with a condenser tube, a mechanical stirrer, and a nitrogen inflow device, with the temperature elevated to 100°C. Once CD10 was completely melted, varying ratios of IA were incorporated, wherein the molar ratios of CD10 to IA ranged from 1:0.8 to 1:1.2, as detailed in Table 1. The temperature was subsequently increased to 160°C, at which point p-toluenesulfonic acid was introduced, and the reaction proceeded under a continuous nitrogen flow for 4 h. Following this, Tin(II) 2-ethylhexanoate was added as a polycondensation catalyst, maintaining the temperature at 160°C while the reaction continued under vacuum for an additional 4 h. Finally, the resultant product was transferred into a container, and NIPUs were obtained through natural cooling at room temperature. NIPUs synthesized with CD10 to IA molar

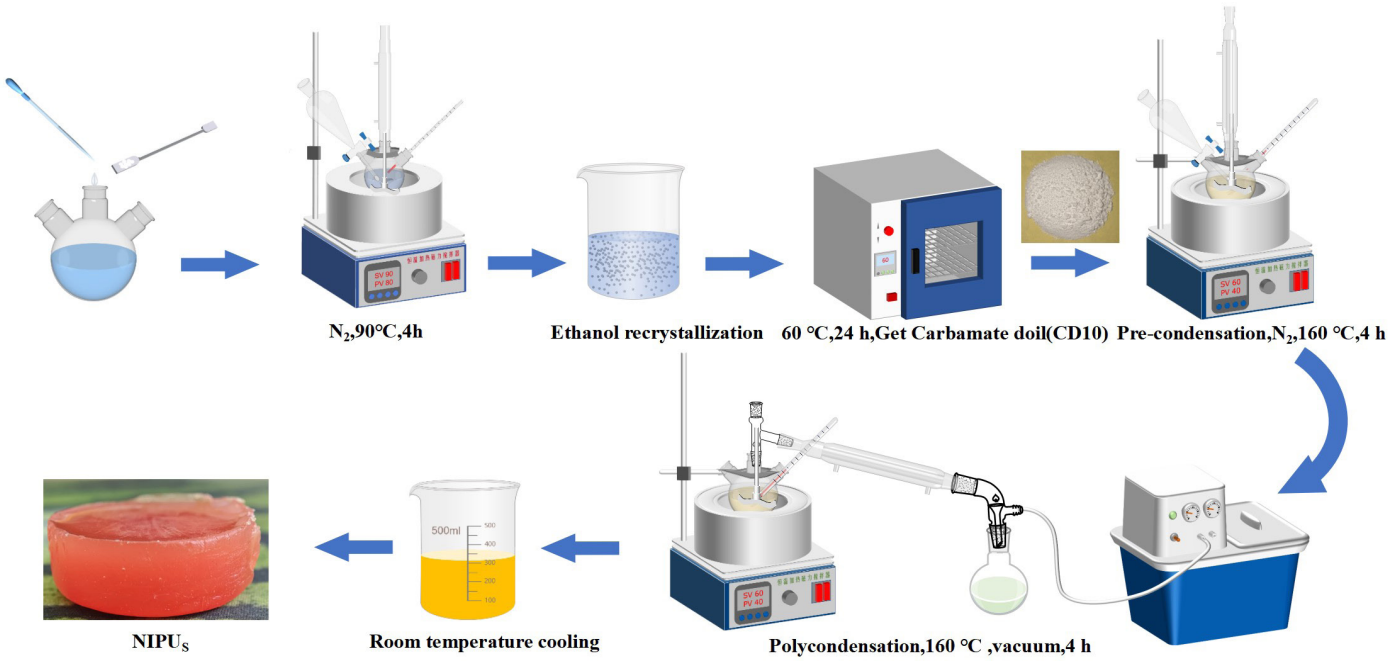

Figure 1. Schematic diagram of the synthesis process of NIPUs.

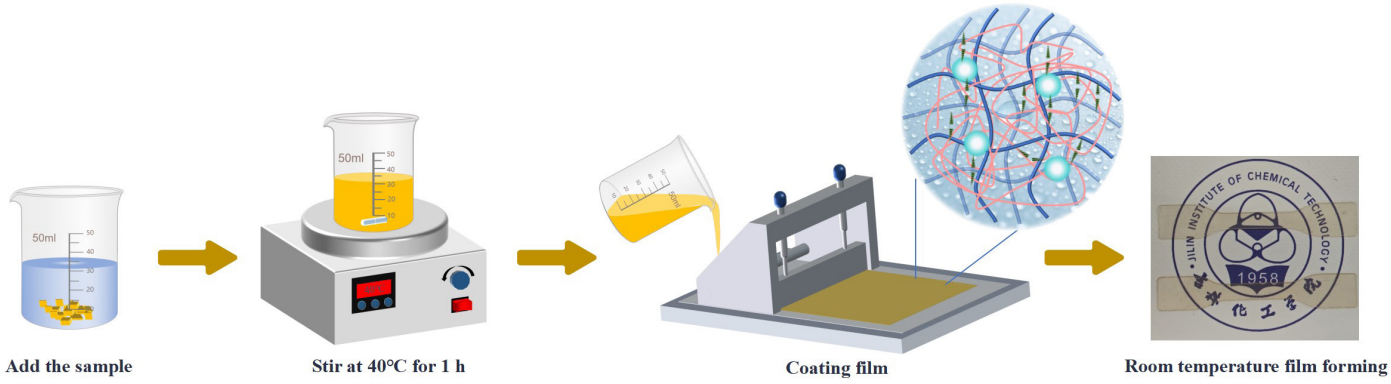

Figure 2. Diagram of the process for making NIPU coating.

ratios ranging from 1:0.8 to 1:1.2 were denoted as $NIPU_{0.8}$, $NIPU_{0.9}$, $NIPU_{1.0}$, $NIPU_{1.1}$, and $NIPU_{1.2}$, respectively. This nomenclature was adopted for clarity in subsequent discussions.

2.3. Preparation of NIPUs coating

As shown in Figure 2, a specific quantity of NIPUs is placed into a beaker, followed by the addition of an appropriate volume of anhydrous EtOH. The mixture was stirred at 40°C for 1 h until the NIPUs completely dissolved. Subsequently, the remaining anhydrous EtOH was added, and the mixture was stirred for an additional 10 min to prepare a NIPU emulsion at 30% concentration. This emulsion was then scraped onto a tinplate using a 50 μm spatula or poured into a latex mold measuring 50 mm × 50 mm × 4 mm. After curing in a clean cabinet at room temperature for 7 days, the film's other properties were tested.

2.4. The methods for NIPUs coating characterization

2.4.1. FT-IR analysis

A small amount of the product was mixed with potassium bromide (KBr) and ground thoroughly. Subsequently, the mixture was pressed into a transparent sheet using a tablet press. The FT-IR spectra were obtained using a WQF-510A FT-IR spectrometer, which scanned the samples 32 times at a resolution of 4 cm^{-1} within the wavenumber range of 500 cm^{-1} to 4000 cm^{-1}.

2.4.2. ^{1}H NMR analysis

Deuterated dimethyl sulfoxide (DMSO-d6) was used as a solvent, and the ^{1}H NMR spectra were generated using a Bruker 600 MHz NMR spectrometer from Germany at room temperature, and structures of the products were determined by analyzing the chemical shifts of the different hydrogens in the spectra.

2.4.3. Thermal stability analysis (TGA)

The thermal stability of the products was tested using a thermogravimetric analyzer model TGA/DSC 3+ from METTLER TOLEDO under a nitrogen atmosphere in the temperature range of 25°C to 700°C with a temperature increase rate of 10°C/min to obtain TGA thermal analysis graphs. All samples were weighed accurately.

2.4.4. Thermal conductivity test

The thermal conductivity of coatings was tested by the transient plane source method using the HCER-S model thermal conductivity tester. The ambient temperature was 20±3°C.

2.4.5. Water absorbency test

The hydrophobic properties of the coating surface were evaluated using a static contact angle meter (J2000DM, Shanghai Zhongchen Digital Technology Equipment Co., Ltd.) under ambient temperature and pressure conditions. A volume of 2.5-5 μL of deionized water was carefully deposited onto three to five distinct locations on the coating surface. The contact angle was recorded once the shape of the droplet stabilized. The average of these measurements was taken as the static contact angle of the coating. To assess the water absorption of the NIPUs coating in accordance with American society for testing and materials (ASTM) standard D570-98, a precisely weighed sample was placed in a sample bottle, to which 20 mL of deionized water was added. After 72 h, the sample was removed, and any surface water was promptly blotted dry with filter paper before being weighed again. In the formula, W_t is the mass of the sample after 72 h of immersion in deionized water, g; W_0 is the initial mass of the sample, g.

Water absorption is calculated by Eq. (1):

$$\text{Water absorption}(\%) = \frac{(w_t - w_0)}{w_0} \times 100\% \quad (1)$$

2.4.6. Coating corrosion resistance test

The corrosion resistance of the coating was evaluated by observing the corrosion on the surface of the substrate after immersing the coated tinplate in 5% NaCl solution for 10 days.

2.4.7. Other performance tests for coatings

According to ASTM D3363, the RW-5101S Electric Pencil Surface Hardness Tester was utilized to assess the hardness of coatings. A sharpened Zhonghua Hardness Test Pencil is affixed to the pencil hardness tester, ensuring that the pencil tip contacts the coating surface. The pencil is then moved unidirectionally across the surface at a speed of 5-10 cm/s for 10 mm. The hardness testing proceeds from the hardest to the softest pencil until the coating surface is no longer scratched by the pencil. The hardness of the coating is indicated by the hardest pencil that fails to scratch the surface. Coating adhesion is evaluated using the grid method, wherein a multi-bladed knife is employed to make perpendicular cuts through the coating, followed by parallel cuts at a 90 ° angle, creating a tic-tac-toe grid pattern. Adhesive tape is applied to the cut coating surface and subsequently removed to assess the level of coating adhesion, in accordance with ISO 12944-6. Furthermore, solvent resistance is tested as per ASTM D1308 by immersing the samples in acid (5% HCl solution), alkali (NaOH solution at pH=8), and organic solvent xylene. The samples are removed every 12 h and dried for 24 h. This process is repeated more than five times, and the weight loss of the samples is recorded and analyzed. Where W_0 is the initial mass of the sample, g; W_d is the mass of the sample after it has been immersed in the solvent for some time and dried, g.

The percentage weight loss is calculated by Eq. (2):

$$\text{Weight loss}(\%) = \frac{(W_0 - W_d)}{W_0} \times 100\% \quad (2)$$

3. Results and Discussion

3.1. Synthesis and structural characterization of CD10

In this section, the reactivity of the nucleophilic reaction diminished due to electron release from the methyl group in PC, which decreases the polarity of the carbonyl bond [10]. Consequently, we modified the reaction conditions based on prior research and successfully synthesized the CD10 through a ring-opening reaction between PC and 1,10-diaminosilane at 90°C for 4 h without the use of any catalyst, as illustrated in Figure 1 [11].

As shown in Figure 3(a), the absorption peak at 1783 cm^{-1}, attributed to the carbonyl (C=O) group of the five-membered cyclic carbonate in PC, completely disappeared upon completion of the reaction. This indicates that the ring-opening reaction of PC occurred due to the nucleophilic attack by the amine groups in DDA on the electrophilic carbonyl carbon in PC, leading to the formation of carbamate groups [43]. The change in the electronic environment surrounding the C=O bond after ring opening resulted in a shift of the absorption peak. The newly formed C=O in the carbamate group was observed at 1678 cm^{-1} in the spectrum of CD10. Additionally, the absorption at 1528 cm^{-1} corresponded to the -NH bending vibration of the carbamate group. The peaks at 2925 cm^{-1} and 2856 cm^{-1} were attributed to the asymmetric and symmetric stretching vibrations of aliphatic -CH_2 groups, respectively [17,44,45].

According to the ^{1}H NMR spectrum shown in Figure 3(b), two signals corresponding to the -NH protons in the carbamate group were observed near 7.0 ppm, indicative of the pseudo-E and Z conformations. The signals at approximately 4.70 ppm correspond to -OH protons, while the signals between 1.03 and 1.09 ppm are attributed to -CH_3 protons. Additionally, the signals in the range of 1.23 to 1.36 ppm correspond to -CH_2 protons in the long chain, and the signal at 2.93 ppm is associated with the -CH_2 protons in CH_2NH. Collectively, these observations confirmed the successful synthesis of CD10.

3.2. Synthesis and characterization of NIPUs

3.2.1. FT-IR and ^{1}H NMR characterization of NIPUs

The FT-IR spectra analysis of NIPUs synthesized with five different ratios of hard chain segments (CD10) and soft chain segments (IA) has been presented in Figure 4(a). In the spectrum, the stretching vibration peaks of -NH and -OH in the carboxyl group appeared around 3318 cm^{-1}. It was observed that these peaks broadened with an increase in the content of soft chain segments. The peak at 1730 cm^{-1} corresponds to the

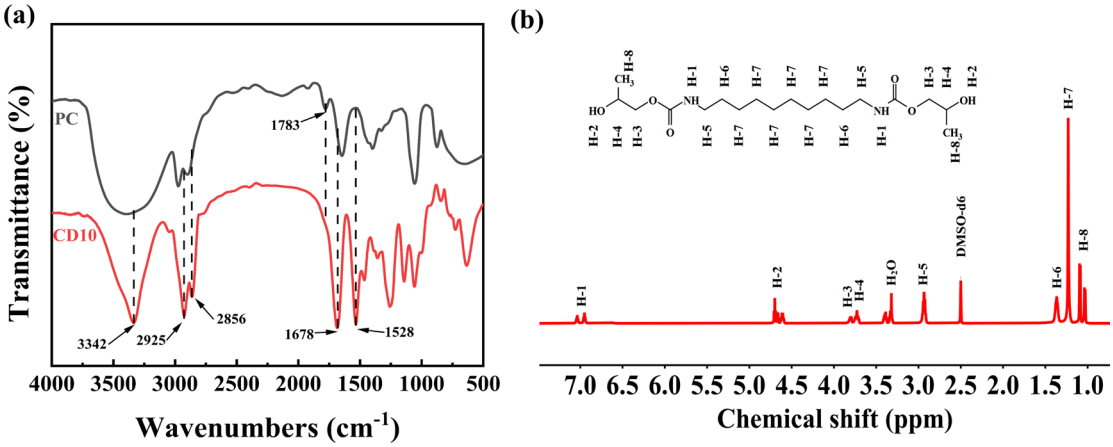

Figure 3. (a) FT-IR and (b) ^{1}H NMR spectra analysis of CD10.

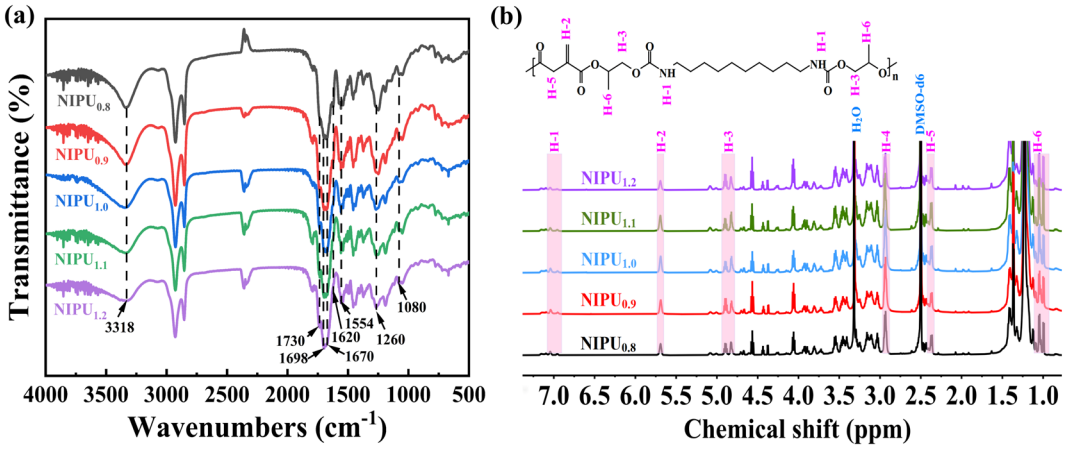

Figure 4. (a) FT-IR and (b) ^{1}H NMR spectra analysis of NIPUs synthesized by mole of different hard segment and soft segment.

C=O in the carboxyl group, while the stretching vibration peaks of C=O in the ester group and C-N/C-O are found at 1698 cm^{-1} and 1260 cm^{-1}, respectively [46]. Additionally, the C=C bond is indicated by a peak at 1670 cm^{-1}, the absorption peak of the δNH amide II band is at 1554 cm^{-1}, and the C-O-C stretching vibration peak is at 1080 cm^{-1}. Notably, the peak at 1620 cm^{-1} represents the absorption band of the urea group. The formation of polyurea occurs when the amount of IA added is less than that of CD10, allowing the remaining CD10 to undergo a self-condensation reaction [9]. However, the figure illustrates that the peak of the urea group gradually diminished as the amount of IA increased, indicating that CD10 reacted more completely with IA, thus forming more ester groups and reducing the occurrence of side reactions.

To further confirm the structure of NIPUs, we characterized them using ^{1}H NMR spectroscopy. The results have been presented in Figure 4(b). The signals with chemical shifts (δ) ranging from 6.96 to 7.04 ppm correspond to the hydrogen atoms in -NH groups, while the signal at 2.37 ppm and the range of 3.50 to 4.50 ppm are attributed to -CH_2 groups between the ester and carbamate functionalities, as well as the -CH_3 protons in the isomer. Additionally, signals near 2.92 ppm are associated with the hydrogen atoms in -CH_2 groups adjacent to -NH groups. The signal with a δ value of 5.69 ppm corresponds to the hydrogen atom of -CH_2 [47]. Based on the results obtained from FT-IR and ^{1}H NMR analyses, we can confirm that both hard chain segments and varying proportions of soft chain segments were successfully synthesized as NIPUs.

3.2.2. Thermal stability of NIPUs

As the substrate resin for coatings, it is crucial to possess a certain degree of thermal stability. Therefore, to investigate the influence of gradually increasing the amount of soft chain segment (IA) on the thermal properties of NIPUs, TGA was employed to assess the thermal degradation behavior of NIPUs. The results, illustrated in Figure 5 and Table 1, indicate that all NIPUs exhibited a similar trend, initiating decomposition around 200°C, with the maximum decomposition temperature reaching approximately 465°C.

As illustrated in Figure 5(b), the thermal decomposition of the synthesized NIPUs proceeded in two distinct stages. The first stage occurred between 250°C and 341°C and was primarily attributed to the cleavage of urethane and ester bonds, which are thermally less stable. The second stage, observed between 458°C and 469°C, corresponded to the degradation of sub-methyl groups in the aliphatic backbone and methyl groups in the side chains [39,47]. As shown in Table 1, the initial decomposition temperature ($T_{5\%}$) decreased from 237°C to 217°C with increasing soft segment content, indicating that a higher proportion of soft segments led to more carbamate groups, which slightly reduced thermal resistance [48]. Meanwhile, the char residue of CD10 was nearly zero, but rose from 4.74% to 8.85% with increasing soft segment content. This suggests that a higher soft segment ratio introduced more urethane groups and promoted hydrogen bonding, thereby enhancing the crosslinking density. However, the char residues of $NIPU_{1.1}$ and $NIPU_{1.2}$ remained relatively constant, implying that beyond a certain soft segment ratio, the hard segments are fully consumed, and further increases do not contribute to additional crosslinking [40]. For reference, Dai [49] *et al.* synthesized three bio-based unsaturated polyesters from IA and various diols, which exhibited 10% weight loss temperatures ranging from 256°C to 295°C and demonstrated good thermal and coating properties. The NIPUs developed in this study exhibit comparable or even superior thermal stability. As evidenced in Figure 5 and Table 1, NIPUs outperformed conventional commercial

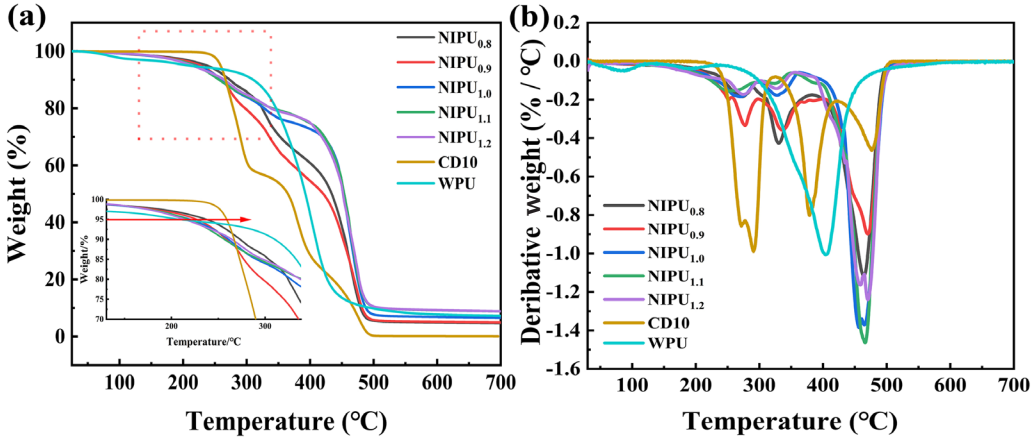

Figure 5. (a) TGA and (b) DTG thermal degradation curves of NIPUs synthesized with different molar ratios of hard and soft segments, compared with CD10 and commercial WPU.

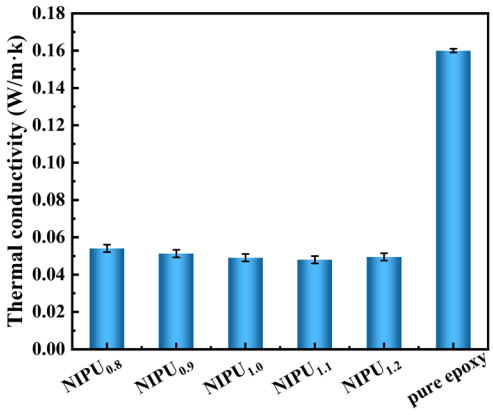

Figure 6. Thermal conductivity of NIPUs synthesized by a mole of different hard and soft segments.

WPU in thermal resistance, underscoring their promise for advanced coating applications. In summary, although soft segment incorporation slightly lowered the onset of thermal degradation, all synthesized NIPUs displayed overall excellent thermal stability.

3.2.3. Thermal conductivity of NIPUs coating

In general, thermal conductivity is a critical measure of a substance's ability to conduct heat, particularly for insulation materials. The NIPU coating was evaluated using the transient planar source method, with results depicted in Figure 6. As the proportion of soft chain segments increased, a greater number of carbamate groups were generated, resulting in enhanced intramolecular and intermolecular hydrogen bonding within the molecule. This led to increased crosslink density; concurrently, thermal resistance rose due to heightened intermolecular interactions [50]. Consequently, the thermal conductivity of the NIPUs coating decreased from 0.0541 to 0.0480. However, when the ratio of soft chain segments to hard chain segments increased to 1.2, the surplus soft chain segments (IA) induced additional side reactions, which decreased the density of urethane groups among the NIPUs molecules. This reduction in crosslink density subsequently caused the thermal conductivity of the NIPUs coating to rise to 0.0495 once more [51]. Compared to traditional pure epoxy resin, the NIPUs coating exhibits lower thermal conductivity, thereby offering enhanced thermal insulation performance, making it a promising candidate for use as a base resin in thermal insulation coatings [52].

3.2.4. Water resistance of NIPUs coating

The water absorption rate and water contact angle are critical indices for evaluating the water resistance of coatings. In this study, the water contact angle and water absorption of NIPUs coating were measured to illustrate changes in their water resistance. The results have been depicted in Figure 7. The data presented in the figure indicates that the water contact angle gradually increased with the rising proportion of soft chain segments. Notably, when the ratio of hard chain segments to soft chain segments was 1:1, the NIPU coating exhibited hydrophobicity. However, optimal hydrophobicity was achieved when this ratio reached 1:1.1, at which point the water contact angle measured 101.49 °, and the corresponding water absorption reached its minimum value of only 1.94%. This phenomenon can be attributed to the presence of hydrophilic -OH groups in CD10. When the quantity of soft chain segments was less than that of hard chain segments, a significant number of -OH groups remained unreacted, facilitating the formation of hydrogen bonds with water molecules. Consequently, the NIPU coating attained strong hydrophilicity [51]. As the number of soft chain segments increased, the carboxyl group (-COOH) reacted with the remaining hydroxyl group (-OH) to form additional carbamate groups. Given that DDA possesses a long aliphatic chain, this results in an increased density of hydrophobic chains within the NIPU coating [53,54]. However, IA, as a soft chain segment, is susceptible to decomposition or side reactions, such as self-condensation, during high-

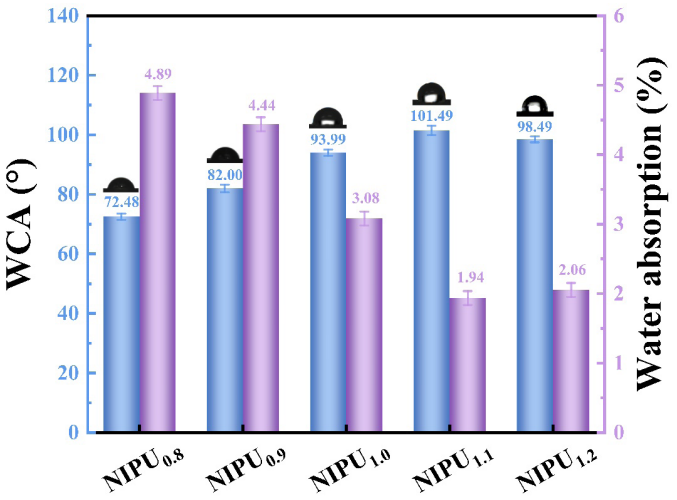

Figure 7. Water contact angle, water contact angle image and water absorption of nipus synthesized with different ratios of soft and hard chains.

temperature reactions. Consequently, when the soft chain segment was slightly overloaded relative to the hard chain segment, the carboxyl and hydroxyl groups available for reaction reached an equilibrium ratio. This maximized the proportion of hydrophilic groups involved in the reaction, leading to a NIPUs coating that exhibited optimal water resistance. Nonetheless, the side reactions of the soft chain segment also released additional hydrophilic groups (-COOH) and generated more by-products, which slightly decreased the cross-linking density and subsequently reduced water resistance [55]. Therefore, the water resistance of $NIPU_{1.2}$ was less in comparison to $NIPU_{1.1}$.

3.2.5. Corrosion resistance of NIPUs coating

The corrosion resistance of the coating was evaluated by immersing the NIPUs-coated tinplate sheets in a 5% NaCl solution for 10 days, as illustrated in Figure 8. The results indicate that the uncoated tinplate sheet exhibited significant corrosion and oxidation following the immersion test. In contrast, the tinplate coated with NIPUs showed minimal corrosion; specifically, the $NIPU_{0.8}$-coated tinplate displayed slight rust and minor peeling, while the coatings of $NIPU_{0.9}$ and $NIPU_{1.0}$ showed small areas of delamination due to water penetration. This phenomenon can be attributed to the insufficient proportion of soft chain segments in the coating, which leads to a higher presence of unreacted hydroxyl groups. The interaction between these hydroxyl groups and water molecules forms hydrogen bonds, thereby weakening the cross-linking with the substrate. Notably, the surfaces of the tinplate coated with $NIPU_{1.1}$ and $NIPU_{1.2}$ exhibited no significant changes. This observation suggested that when the ratio of hard chain segments to soft chain segments reached 1:1.1, the cross-link density of the coating

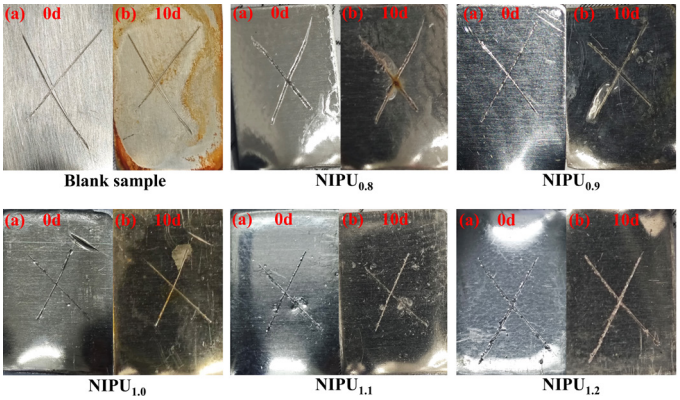

Figure 8. Corrosion resistance of NIPUs coating: (a) coating before treatment; (b) corresponding coating after immersion in 5% NaCl solution for 10 days.

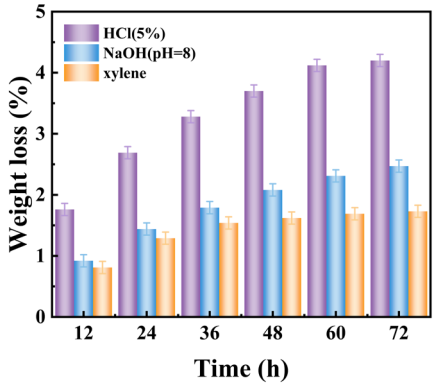

Figure 9. Anticorrosion mechanism of NIPUs coating.

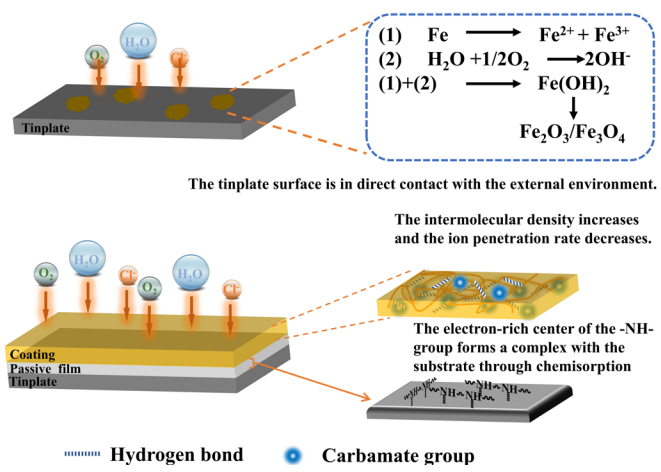

Figure 10. Solubility of $NIPU_{1.1}$ in HCl (5%), NaOH (pH = 8), and xylene.

Table 2. Basic appearance and mechanical properties of NIPUs coating.

NIPUs	Film-forming or not	Tack-free time(h)	Coating appearance	Coating thickness (μm)	Pencil hardness[a]	Adhesion[b]
CD10	No	—	Mass fragmentation	—	—	—
$NIPU_{0.8}$	Yes	8	Cracks, slightly yellow, and transparent	200	2H	0
$NIPU_{0.9}$	Yes	8	Flat, slightly yellow, and transparent	200	2H	0
$NIPU_{1.0}$	Yes	8	Flat, slightly yellow, and transparent	200	H	0
$NIPU_{1.1}$	Yes	10	Flat, slightly yellow, and transparent	200	H	0
$NIPU_{1.2}$	Yes	10	Flat, slightly yellow, and transparent	200	HB	0

[a]Measured according to ASTM D3363.
[b]Measured according to ISO 12944-6, the test is conducted using the grid method.

was optimized, effectively preventing corrosive media from penetrating the coating and thereby endowing the NIPU coating with excellent corrosion resistance [40]. According to previous reports, a series of waterborne PUs were prepared [56], coated on tinplate, soaked in 5% NaCl solution for 72 h, and all the tinplates showed rust. When aluminum alloy sheets coated with traditional epoxy resin were soaked in 5% NaCl solution for 7 days, signs of corrosion spots were evident [57]. In contrast, our study showed better anti-corrosion properties.

The corrosion protection mechanism of NIPUs has been illustrated in Figure 9. In the absence of a protective coating, the metal surface (Fe) is directly exposed to the external environment, resulting in a reaction with hydroxide ions that forms iron oxide [58]. The incorporation of IA leads to a progressive increase in the density of carbamate groups. The strong intramolecular hydrogen bonding significantly enhances the development of a well-adhered, uniform, and dense coating structure. This, in turn, prolongs ion penetration time and substantially improves corrosion resistance [59,60]. Additionally, the electron-rich center of the amide group (NH) in the polymer main chain can form a complex with the substrate through chemisorption, thereby establishing a protective layer [61].

3.2.6. Other properties of NIPUs coating

The basic properties of the coatings have been summarized in Table 2. It is evident that when CD10 was not modified with IA, it could not form a coating due to its inherent rigidity. Furthermore, acid and alkali resistance, solvent resistance, pencil hardness, and adhesion are critical indicators for assessing the overall performance of the coating. In this study, tests for acid and alkali resistance, as well as solvent resistance, were conducted using the $NIPU_{1.1}$ coating as a specimen, with the results illustrated in Figure 10. The coating was evaluated in environments containing acid, alkali, and organic solvents, where $NIPU_{1.1}$ exhibited the highest weight loss in a 5% HCl solution. This phenomenon may be attributed to the ability of the HCl solution to diffuse more readily into the ester bond structure within the cured film, leading to hydrolysis of the ester bonds [62]. Nevertheless, $NIPU_{1.1}$ demonstrated overall good resistance to both acids and alkalis, as well as to organic solvents. The hardness of NIPUs coating was primarily influenced by two factors: the crosslink density of the curing system and the molecular structure of the system [63].

From the data presented in Table 2, it is evident that the pencil hardness of the coating decreased as the proportion of soft chain segments increased. This phenomenon can be attributed to the presence of a side-chain methyl group in PC, which contributes to the synthesis of hard chain segments that contain a greater number of bulky methyl groups. These bulky groups enhance the rigidity and scratch resistance of the NIPUs. However, an increase in the proportion of soft chain segments results in a reduction of this rigidity [14]. Notably, all five different ratios of NIPUs exhibited superior adhesion properties, attributed to the abundance of polar groups (e.g., urethane groups, remaining hydroxyl groups, etc.) that facilitate the formation of numerous intermolecular hydrogen bonds between the coating and the substrate.

4. Conclusions

In this study, the polycondensation of NIPUs was conducted at various molar ratios ranging from 1:0.8 to 1:1.2 for hard (CD10) and soft chain segments (IA). The successful synthesis of the desired NIPUs from all five feedstock ratios was confirmed using FT-IR and ^1H NMR analyses. An analysis of the thermal stability of NIPUs revealed that an increase in the proportion of soft chain segments had a minimal effect on the thermal stability of the polymer coating. The thermal conductivity and water resistance of NIPUs coatings were evaluated, revealing that a hard-to-soft chain segment ratio of 1:1.1 yielded the lowest thermal conductivity and the highest water contact angle. This outcome is attributed to the maximization of the ratio of hydroxyl and carboxyl groups involved in the reaction, resulting in the highest cross-linking density, which in turn led to the coatings exhibiting superior thermal insulation and water resistance. When the ratio of soft segment chains exceeds 1:1.1, the excess soft segment chain is prone to side reactions, resulting in a decrease in the crosslink density of the coating, which consequently reduces its relevant properties. Furthermore, when the

ratio of hard chain segments to soft chain segments reaches 1:1.1, the tinplate coated with NIPUs exhibits no signs of corrosion, demonstrating significant corrosion resistance. Lastly, the coating was evaluated for solvent resistance, pencil hardness, and adhesion, and was found to perform well in these tests. The synthesis of NIPUs coating in this study is straightforward, does not require high-temperature curing or expensive catalysts, is easy to apply in industrial settings, and underscores the potential value of biobased NIPU polymers for developing applications suitable for thermal insulation and anticorrosive coating matrices.

CRediT authorship contribution statement

Bin Chen: Methodology, Software, Validation, Writing - Original Draft, Formal analysis. **Xu Wang:** Data curation, Resources. **Haoran Xu:** Visualization, Investigation. **Yu Zhang:** Software, Validation, Writing- Reviewing and Editing. **Chengqian Wang:** Conceptualization, Supervision, Software, Validation, Writing - Reviewing and Editing, Funding acquisition.

Declaration of competing interest

The authors declare that they have no known competing financial interests or personal relationships that could have appeared to influence the work reported in this paper.

Declaration of Generative AI and AI-assisted technologies in the writing process

The authors confirm that there was no use of artificial intelligence (AI)-assisted technology for assisting in the writing or editing of the manuscript and no images were manipulated using AI.

Acknowledgment

This research was supported by grants from the Doctor Startup Foundation of the Jilin Institute of Chemical Technology (Number: 2022012).

The authors acknowledge the assistance of JLICT Center of Characterization and Analysis.

References

1. Akindoyo, J.O., Beg, M.D.H., Ghazali, S., Islam, M.R., Jeyaratnam, N., Yuvaraj, A.R., 2016. Polyurethane types, synthesis and applications – A review. *RSC Advances*, **6**, 114453-114482. https://doi.org/10.1039/c6ra14525f
2. Jing, Q., Liu, Q., Li, L., Dong, Z.L., Silberschmidt, V.V., 2016. Effect of graphene-oxide enhancement on large-deflection bending performance of thermoplastic polyurethane elastomer. *Composites Part B: Engineering*, **89**, 1-8. https://doi.org/10.1016/j.compositesb.2015.11.033
3. Mazari, F., Chotebor, M., Naeem, J., Mazari, A., Havelka, A., 2016. Effect of perforated polyurethane foam on moisture permeability for car seat comfort. *Fibres and Textiles in Eastern Europe*, **24**, 165-169. https://doi.org/10.5604/12303666.1221752
4. Zhang, Z., Han, X., Jia, L., Yu, W., Zheng, Q., 2024. Highly water-resistant transparent waterborne polyurethane thermal-insulation coating material with multiple self-crosslinking network based on controllably activated end-capping reagent. *Progress in Organic Coatings*, **187**, 108104. https://doi.org/10.1016/j.porgcoat.2023.108104
5. Ghasemlou, M., Daver, F., Ivanova, E.P., Adhikari, B., 2019. Bio-based routes to synthesize cyclic carbonates and polyamines precursors of non-isocyanate polyurethanes: A review. *European Polymer Journal*, **118**, 668-684. https://doi.org/10.1016/j.eurpolymj.2019.06.032
6. Nohra, B., Candy, L., Blanco, J.-F., Guerin, C., Raoul, Y., Mouloungui, Z., 2013. From petrochemical polyurethanes to biobased polyhydroxyurethanes. *Macromolecules*, **46**, 3771-3792. https://doi.org/10.1021/ma400197c
7. Cornille, A., Auvergne, R., Figovsky, O., Boutevin, B., Caillol, S., 2017. A perspective approach to sustainable routes for non-isocyanate polyurethanes. *European Polymer Journal*, **87**, 535-552. https://doi.org/10.1016/j.eurpolymj.2016.11.027
8. Ochiai, B., Utsuno, T., 2013. Non-isocyanate synthesis and application of telechelic polyurethanes via polycondensation of diurethanes obtained from ethylene carbonate and diamines. *Journal of Polymer Science Part A: Polymer Chemistry*, **51**, 525-533. https://doi.org/10.1002/pola.26418
9. Rokicki, G., Piotrowska, A., 2002. A new route to polyurethanes from ethylene carbonate, diamines and diols. *Polymer*, **43**, 2927-2935. https://doi.org/10.1016/s0032-3861(02)00071-x
10. Singh, N., Bakhshi, H., Meyer, W., 2020. Developing non-isocyanate urethane-methacrylate photo-monomers for 3D printing application. *RSC Advances*, **10**, 44103-44110. https://doi.org/10.1039/d0ra06388f
11. Kotanen, S., Wirtanen, T., Mahlberg, R., Anghelescu-Hakala, A., Harjunalanen, T., Willberg-Keyrilainen, P., Laaksonen, T., Sarlin, E., 2023. Cyclic carbonates as building blocks for non-isocyanate polyurethanes. *Journal of Applied Polymer Science*, **140**, e53964. https://doi.org/10.1002/app.53964
12. Suqing, L., Jingbo, Z., Zhiyuan, Z., Junying, Z., Wantai, Y., 2017. Influence of crystallizable units on the properties of aliphatic thermoplastic poly(ether urethane) s synthesized through a non-isocyanate route. *Journal of Elastomers & Plastics*, **49**, 738-757. https://doi.org/10.1177/0095244317695363
13. Ochiai, B., Inoue, S., Endo, T., 2005. Salt effect on polyaddition of bifunctional cyclic carbonate and diamine. *Journal of Polymer Science Part A: Polymer Chemistry*, **43**, 6282-6286. https://doi.org/10.1002/pola.21081
14. Kotanen, S., Laurikainen, P., Lehtimäki, S., Harjunalanen, T., Laaksonen, T., Sarlin, E., 2024. The role of hard and soft segments in the thermal and mechanical properties of non-isocyanate polyurethanes produced via polycondensation reaction. *International Journal of Adhesion and Adhesives*, **132**, 103726. https://doi.org/10.1016/j.ijadhadh.2024.103726
15. Deepa, P., Jayakannan, M., 2008. Solvent-free and nonisocyanate melt transurethane reaction for aliphatic polyurethanes and mechanistic aspects. *Journal of Polymer Science Part A: Polymer Chemistry*, **46**, 2445-2458. https://doi.org/10.1002/pola.22578
16. Wołosz, D., Parzuchowski, P.G., Świderska, A., 2021. Synthesis and characterization of the non-isocyanate poly(carbonate-urethane)s obtained via polycondensation route. *European Polymer Journal*, **155**, 110574. https://doi.org/10.1016/j.eurpolymj.2021.110574
17. Wołosz, D., Parzuchowski, P.G., Rolińska, K., 2022. Environmentally Friendly Synthesis of Urea-Free Poly(carbonate-urethane) Elastomers. *Macromolecules*, **55**, 4995-5008. https://doi.org/10.1021/acs.macromol.2c00706
18. Shen, Z., Zheng, L., Song, D., Liu, Y., Li, C., Liu, J., Xiao, Y., Wu, S., Zhou, T., Zhang, B., Lv, X., Mei, Q., 2022. A non-isocyanate route to poly(Ether Urethane): Synthesis and effect of chemical structures of hard segment. *Polymers*, **14**, 2039. https://doi.org/10.3390/polym14102039
19. Wu, Z., Cai, W., Chen, R., Qu, J., 2018. Synthesis and properties of ambient-curable non-isocyanate polyurethanes. *Progress in Organic Coatings*, **119**, 116-122. https://doi.org/10.1016/j.porgcoat.2018.02.006
20. Zhang, C., Huang, K.C., Wang, H., Zhou, Q., 2020. Anti-corrosion non-isocyanate polyurethane polysiloxane organic/inorganic hybrid coatings. *Progress in Organic Coatings*, **148**, 105855-105122. https://doi.org/10.1016/j.porgcoat.2020.105855
21. Tryznowski, M., Izdebska-Podsiadły, J., Żołek-Tryznowska, Z., 2017. Wettability and surface free energy of NIPU coatings based on bis(2,3-dihydroxypropyl)ether dicarbonate. *Progress in Organic Coatings*, **109**, 55-60. https://doi.org/10.1016/j.porgcoat.2017.04.011
22. Khatoon, H., Iqbal, S., Irfan, M., Darda, A., Rawat, N.K., 2021. A review on the production, properties and applications of non-isocyanate polyurethane: A greener perspective. *Progress in Organic Coatings*, **154**, 106124. https://doi.org/10.1016/j.porgcoat.2020.106124
23. Pathak, R., Kathalewar, M., Wazarkar, K., Sabnis, A., 2015. Non-isocyanate polyurethane (NIPU) from tris-2-hydroxy ethyl isocyanurate modified fatty acid for coating applications. *Progress in Organic Coatings*, **89**, 160-169. https://doi.org/10.1016/j.porgcoat.2015.08.015
24. Zhang, P., Zhang, G., Pan, J., Ma, C., Zhang, G., 2023. Non-isocyanate polyurethane coating with high hardness, superior flexibility, and strong substrate adhesion. *ACS Applied Materials & Interfaces*, **15**, 5998-6004. https://doi.org/10.1021/acsami.2c22433
25. Liu, C., Wu, J., Zhou, X., Zhou, X., Wu, Z., Qu, J., 2022. Synthesis and properties of poly(dimethylsiloxane)-based non-isocyanate polyurethanes coatings with good anti-smudge properties. *Progress in Organic Coatings*, **163**, 106690. https://doi.org/10.1016/j.porgcoat.2021.106690
26. Liu, G., Wu, G., Huo, S., Jin, C., Kong, Z., 2017. Synthesis and properties of non-isocyanate polyurethane coatings derived from cyclic carbonate-functionalized polysiloxanes. *Progress in Organic Coatings*, **112**, 169-175. https://doi.org/10.1016/j.porgcoat.2017.07.013
27. Asemani, H.R., Mannari, V., 2019. Synthesis and evaluation of non-isocyanate polyurethane polyols for heat-cured thermoset coatings. *Progress in Organic Coatings*, **131**, 247-258. https://doi.org/10.1016/j.porgcoat.2019.02.036
28. Bähr, M., Mülhaupt, R., 2012. Linseed and soybean oil-based polyurethanes prepared via the non-isocyanate route and catalytic carbon dioxide conversion. *Green Chemistry*, **14**, 483. https://doi.org/10.1039/c2gc16230j
29. Kathalewar, M., Sabnis, A., D'Melo, D., 2014. Polyurethane coatings prepared from CNSL based polyols: Synthesis, characterization and properties. *Progress in Organic Coatings*, **77**, 616-626. https://doi.org/10.1016/j.porgcoat.2013.11.028
30. Karami, Z., Zohuriaan-Mehr, M.J., Rostami, A., 2017. Bio-based thermo-healable non-isocyanate polyurethane DA network in comparison with its epoxy counterpart. *Journal of CO2 Utilization*, **18**, 294-302. https://doi.org/10.1016/j.jcou.2017.02.009
31. Bähr, M., Bitto, A., Mülhaupt, R., 2012. Cyclic limonene dicarbonate as a new monomer for non-isocyanate oligo- and polyurethanes (NIPU) based upon terpenes. *Green Chemistry*, **14**, 1447. https://doi.org/10.1039/c2gc35099h
32. Schmidt, S., Ritter, B.S., Kratzert, D., Bruchmann, B., Mülhaupt, R., 2016. Isocyanate-free route to poly(carbohydrate–urethane) thermosets and 100% bio-based coatings derived from glycerol feedstock. *Macromolecules*. **49**, 7268-7276. https://doi.org/10.1021/acs.macromol.6b01485
33. Choong, P.S., Chong, N.X., Wai Tam, E.K., Seayad, A.M., Seayad, J., Jana, S., 2021. Biobased nonisocyanate polyurethanes as recyclable and intrinsic self-healing

coating with triple healing sites. *ACS Macro Letters*, **10**, 635-641. https://doi.org/10.1021/acsmacrolett.1c00163
34. Dai, J., Ma, S., Liu, X., Han, L., Wu, Y., Dai, X., Zhu, J., 2015. Synthesis of bio-based unsaturated polyester resins and their application in waterborne UV-curable coatings. *Progress in Organic Coatings*, **78**, 49-54. https://doi.org/10.1016/j.porgcoat.2014.10.007
35. Dai, Z.H., Yang, Z.W., Chen, Z.W., Zhao, Z.X., Lou, Y.J., Zhang, Y.Y., Liu, T.X., Fu, F.Y., Fu, Y.Q., Liu, X.D., 2018. Fully biobased composites of an itaconic acid derived unsaturated polyester reinforced with cotton fabrics. *ACS Sustainable Chemistry & Engineering*, **6**, 15056-15063. https://doi.org/10.1021/acssuschemeng.8b03539
36. Melilli, G., Guigo, N., Robert, T., Sbirrazzuoli, N., 2022. Radical oxidation of itaconic acid-derived unsaturated polyesters under thermal curing conditions. *Macromolecules*, **55**, 9011-9021. https://doi.org/10.1021/acs.macromol.2c01682
37. Feng, C., Ma, H., Ren, F., Zhou, Z., Xu, W., 2023. Synthesis of fully bio-based branched unsaturated polyester oligomers and UV curing coatings. *Journal of Coatings Technology and Research*, **20**, 1747-1758. https://doi.org/10.1007/s11998-023-00778-3
38. Huang, Y., Zhou, Q., Li, L., Wang, Q., Guo, C., 2023. Construction of waterborne flame-retardant itaconate-based unsaturated polyesters and application for UV-curable hybrid coatings on wood. *Progress in Organic Coatings*, **183**, 107826-101758. https://doi.org/10.1016/j.porgcoat.2023.107826
39. Ling, Z., Zhou, Q., 2023. Synthesis and properties of linseed oil-based waterborne non-isocyanate polyurethane coating. *Green Chemistry*, **25**, 10082-10090. https://doi.org/10.1039/d3gc03249c
40. Choong, P.S., Rusli, W., Seayad, A.M., Seayad, J., Jana, S., 2024. Crosslinked succinic acid based non-isocyanate polyurethanes for corrosion resistant protective coatings. *Progress in Organic Coatings*, **186**, 107961. https://doi.org/10.1016/j.porgcoat.2023.107961
41. Pouladi, J., Mirabedini, S.M., Eivaz Mohammadloo, H., Rad, N.G., 2021. Synthesis of novel plant oil-based isocyanate-free urethane coatings and study of their anti-corrosion properties. *European Polymer Journal*, **153**, 110502. https://doi.org/10.1016/j.eurpolymj.2021.110502
42. Wang, Z., Wei, T., Xue, X., He, M., Xue, J., Song, M., Wu, S., Kang, H., Zhang, L., Jia, Q., 2014. Synthesis of fully bio-based polyamides with tunable properties by employing itaconic acid. *Polymer*, **55**, 4846-4856. https://doi.org/10.1016/j.polymer.2014.07.034
43. Rayung, M., Ghani, N.A., Hasanudin, N., 2024. A review on vegetable oil-based non isocyanate polyurethane: Towards a greener and sustainable production route. *RSC Advances*, **14**, 9273-9299. https://doi.org/10.1039/d3ra08684d
44. Bossion, A., Aguirresarobe, R.H., Irusta, L., Taton, D., Cramail, H., Grau, E., Mecerreyes, D., Su, C., Liu, G., Müller, A.J., Sardon, H., 2018. Unexpected synthesis of segmented poly(hydroxyurea–urethane)s from dicyclic carbonates and diamines by organocatalysis. *Macromolecules*, **51**, 5556-5566. https://doi.org/10.1021/acs.macromol.8b00731
45. Günther, F., Batista Simões, M., Imasato, H., Pereira Rodrigues-Filho, U., 2019. Experimental and theoretical assessment of the aminolysis of cyclo carbonate to form polyhydroxyurethanes. *Materials Today Communications*, **21**, 100604. https://doi.org/10.1016/j.mtcomm.2019.100604
46. He, X., Xu, X., Wan, Q., Bo, G., Yan, Y., 2019. Solvent- and catalyst-free synthesis, hybridization and characterization of biobased nonisocyanate polyurethane (NIPU). *Polymers*, **11**, 1026. https://doi.org/10.3390/polym11061026
47. Wang, Z., Zhang, X., Zhang, L., Tan, T., Fong, H., 2016. Nonisocyanate biobased poly(ester urethanes) with tunable properties synthesized via an environment-friendly route. *ACS Sustainable Chemistry & Engineering*, **4**, 2762-2770. https://doi.org/10.1021/acssuschemeng.6b00275
48. Lu, Y., Larock, R.C., 2008. Soybean-oil-based waterborne polyurethane dispersions: Effects of polyol functionality and hard segment content on properties. *Biomacromolecules*, **9**, 3332-3340. https://doi.org/10.1021/bm801030g
49. Dai, J., Ma, S., Wu, Y., Han, L., Zhang, L., Zhu, J., Liu, X., 2015. Polyesters derived from itaconic acid for the properties and bio-based content enhancement of soybean oil-based thermosets. *Green Chemistry*, **17**, 2383-2392. https://doi.org/10.1039/c4gc02057j
50. Bamane, P.B., Wadgaonkar, K.K., Chambhare, S.U., Mehta, L.B., Jagtap, R.N., 2020. Replacement of traditional unsaturated acid by bio-based itaconic acid in the preparation of isophthalic acid-based unsaturated polyester resin. *Progress in Organic Coatings*, **147**, 105743. https://doi.org/10.1016/j.porgcoat.2020.105743
51. Papadopoulos, L., Kluge, M., Bikiaris, D.N., Robert, T., 2020. Straightforward synthetic protocol to bio-basedunsaturated poly(ester amide)s from itaconic acidwith thixotropic behavior. *Polymers*, **12**, 980. https://doi.org/10.3390/polym12040980
52. Yang, Z., Yu, S., Sun, W., Xing, Z., Gao, W., Wang, L., Nie, X., Li, W., Liu, G., 2022. High-efficiency preparation of reduced graphene oxide by a two-step reduction method and its synergistic enhancement of thermally conductive and anticorrosive performance for epoxy coatings. *Industrial & Engineering Chemistry Research*, **61**, 3044-3054. https://doi.org/10.1021/acs.iecr.1c04257
53. Oladzadabbasabadi, N., Abraham, B., Ghasemlou, M., Ivanova, E.P., Adhikari, B., 2024. Green synthesis of non-isocyanate hydroxyurethane and its hybridization with carboxymethyl cellulose to produce films. *International Journal of Biological Macromolecules*, **276**, 133617. https://doi.org/10.1016/j.ijbiomac.2024.133617
54. Ghasemlou, M., Daver, F., Ivanova, E.P., Adhikari, B., 2020. Synthesis of green hybrid materials using starch and non-isocyanate polyurethanes. *Carbohydrate Polymers*, **229**, 115535. https://doi.org/10.1016/j.carbpol.2019.115535
55. Tai, N.L., Adhikari, R., Shanks, R., Adhikari, B., 2017. Flexible starch-polyurethane films: Physiochemical characteristics and hydrophobicity. *Carbohydrate Polymers*, **163**, 236-246. https://doi.org/10.1016/j.carbpol.2017.01.082
56. Zhang, J., Zhai, R., Li, J., Hong, C., Xu, Y., Chen, M., Zhou, C., 2025. Benzimidazole functionalized waterborne polyurethane with excellent mechanical properties, UV and corrosion resistance. *Progress in Organic Coatings*, **199**, 108945. https://doi.org/10.1016/j.porgcoat.2024.108945
57. Huang, Y., Yan, H., Cai, M., Song, S., He, C., Fan, X., Zhu, M., 2022. Polyurea as a reinforcing filler for the anti-corrosion and wear-resistant application of epoxy resin. *Progress in Organic Coatings*, **171**, 107049. https://doi.org/10.1016/j.porgcoat.2022.107049
58. Daei, F., Seyed Dorraji, M.S., Azizi, M., Rastgar, M., Naeini, P.S., 2024. Outstanding performance of flower-like NiO nanostructures in epoxied soybean oil-based polyurethane nanocomposite coatings: Investigation of anticorrosion and antibacterial properties. *Colloids and Surfaces A: Physicochemical and Engineering Aspects*, **692**, 133943. https://doi.org/10.1016/j.colsurfa.2024.133943
59. Khatoon, H., Ahmad, S., 2019. Vanadium pentoxide-enwrapped polydiphenylamine/polyurethane nanocomposite: High-performance anticorrosive coating. *ACS Applied Materials & Interfaces*, **11**, 2374-2385. https://doi.org/10.1021/acsami.8b17861
60. Jin, T., Zhang, Q., Yin, H., Cole, I.S., Zhao, P., Wang, Y., Liu, X., 2020. Corrosion resistance of itaconic acid doped polyaniline/nanographene oxide composite coating. *Nanotechnology*, **31**, 285704. https://doi.org/10.1088/1361-6528/ab824a
61. Youssef, E.A.M., 2004. Preparation and characterisation of high performance anticorrosive paints based on novel corrosion inhibitive amide polymers. *Pigment & Resin Technology*, **33**, 152-159. https://doi.org/10.1108/03699420410537269
62. Wei, D., Liao, B., Yong, Q., Wang, H., Li, T., Huang, J., Pang, H., 2019. Castor oil-based waterborne hyperbranched polyurethane acrylate emulsion for UV-curable coatings with excellent chemical resistance and high hardness. *Journal of Coatings Technology and Research*, **16**, 415-428. https://doi.org/10.1007/s11998-018-0120-1
63. Bayramoğlu, G., Kahraman, M.V., Kayaman-Apohan, N., Güngör, A., 2007. The coating performance of adipic acid modified and methacrylated bisphenol- A based epoxy oligomers. *Polymers for Advanced Technologies*, **18**, 173-179. https://doi.org/10.1002/pat.809